This is an *Accepted Manuscript*, which has been through the
Royal Society of Chemistry peer review process and has been
accepted for publication.

Accepted Manuscripts are published online shortly after
acceptance, before technical editing, formatting and proof reading.
Using this free service, authors can make their results available
to the community, in citable form, before we publish the edited
article. We will replace this *Accepted Manuscript* with the edited
and formatted *Advance Article* as soon as it is available.

You can find more information about *Accepted Manuscripts* in the
Information for Authors.

Please note that technical editing may introduce minor changes
to the text and/or graphics, which may alter content. The journal's
standard **Terms & Conditions** and the **Ethical guidelines** still
apply. In no event shall the Royal Society of Chemistry be held
responsible for any errors or omissions in this *Accepted Manuscript*
or any consequences arising from the use of any information it
contains.

Journal Name

Dynamic Article Links ▶

ARTICLE TYPE

Self-setting bioceramic microscopic protrusions for transdermal drug delivery

Bing Cai, Wei Xia*, Susanne Bredenberg, Håkan Engqvist

Microneedle (MN) technology offers a both efficient and minimal invasive transdermal drug delivery strategy. The current MNs, made of silicon and metal, have poor biocompatibility and low drug loading, while the polymer MNs have some constrains related to mechanical strength and storage conditions. In this study, self-setting bioceramics were explored as substitutes for the current MN materials for the first
10 time. Self-setting bioceramic microneedles were fabricated using a master mold by a procedure under mild conditions, which could minimize the drug degradation during fabrication and also facilitates a high drug loading capability than the other current ceramic microneedles. The drug release and mechanical strength was correlated to the microstructure and porosity of the needles. As, observed by SEM and microCT, the ceramic paste could fully fill the geometry of the mould and was cured into an array of
15 micro-sized needles. The drug release study showed that the release rate from this type of MN array could be controlled by the bulk surface area, porosity and resorption rate of the ceramic needles. Applying the MN's to porcine skin indicated that the needles were able to pierce the stratum corneum of the skin. We successfully prepared the bioceramic needles that have high mechanical strength and are resorbable, which can promote safe, efficient and successful transdermal drug delivery.

Introduction

Microneedle (MN) technology (in this study, the term microneedle is used to describe arrays of microscopic protrusions) offers an exciting transdermal drug delivery strategy that can be used to breach the barrier function of the stratum
25 corneum in order to transport charged or large-molecular-weight drugs through the skin more efficiently than conventional transdermal patches. Such small (measured in micrometers) needles could reduce the risk of stimulating nerve endings and piercing capillaries during insertion, thus minimizing pain and
30 infection (**Figure 1**a).[1-3] However, the design of a safe, effective MN system imposes heavy demands on the needle material. Various materials, such as silicon, metals and polymers, have been investigated for use in MN applications in recent decades.[4-9] Microneedles made of silicon and metal are limited by the
35 amount of drug loading and high expenses of manufacturing.[10] Polymers could easily be molded into microneedles but have limitations in mechanical strength, limited storage conditions and degradation of incorporated drugs during fabrication process.[10] The development of suitable material for microneedle array is
40 significantly driven by the rapidly increasing interest in the field of transdermal drug delivery with minimal invasion. Ceramics could be promising in this respect, because of their advantageous properties; they are mechanically strong and biocompatible, and they offer controlled porosity and easy handling during the
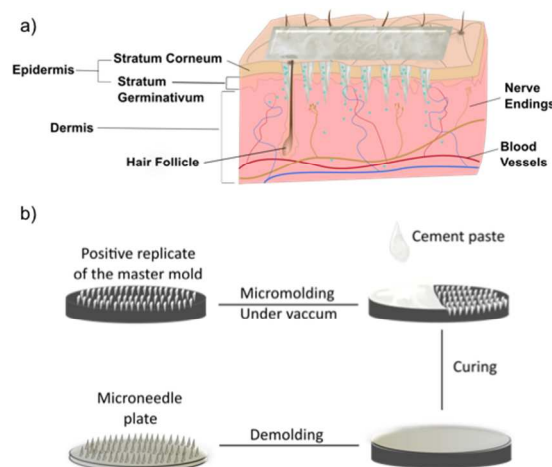45 production process. Their adjustable porosity and the electrostatic

Figure 1 a) Illustration of microneedles (MNs) inserting into skin. The MNs pierce through the stratum corneum to deliver drug more efficiently than traditional transdermal patches. b) Illustration of the production process for self-setting ceramic (SC) MNs. The premixed
50 ceramic paste, with or without drugs, was placed into the positive replicate of the master mold and the cavities were filled under vaccum. The SCMN plate was then cured and demolded carefully. The SCMN plates were air-dried before testing.

interaction between the ceramic surface and the transported drugs
55 have been widely studied and utilized in a broad range of biomedical applications to control drug release.[11]

To our knowledge, only one ceramic, alumina, has been evaluated as an MN material. It has been shown that ceramic

(alumina) MNs have sufficient mechanical strength to remain intact during insertion through the dermis.[12, 13] Alumina needles have also delivered test compounds through the skin in an *ex vivo* human skin model.[13] However, extreme conditions involving sintering at high temperature were used to make these MNs, thus precluding the incorporation of drug into the ceramic material before molding it into the needles. Instead, the drug was loaded by dipping the needles into a concentrated drug solution, a process that was associated with limited loading capacity, release behavior and applications. In another study, stainless steel MNs were coated with porous calcium phosphate to improve the drug-release behavior and increase the drug loading capacity.[14] However, the drug loading was still limited.

At present, there are no published studies showing that ceramic MNs could fulfil the drug-loading and controlled-release criteria for transdermal drug delivery. However, the use of self-setting ceramics could provide a solution to the problem of drug loading. A self-setting, fluid, cohesive ceramic paste loaded with drug could be molded into the desired shape at room temperature. The process would occur under mild conditions that would limit degradation of the drug and thus offer more flexibility for drug-loading, i.e. the drug content (and thus the dose) could be adjusted without having to take the solubility, molecular size, and polarity of the drug into consideration. Well-known self-setting bioceramics, such as calcium sulfate dihydrate [gypsum $(CaSO_4 \cdot 2H_2O)$; CaS] and calcium phosphate dihydrate [brushite $(CaHPO_4 \cdot 2H_2O)$; CaP], have drug carrying ability and sufficient mechanical strength for the task.[15-19] The resorbability and biocompatibility of gypsum and brushite as bone substitution materials have been validated in many *in vivo* and clinical tests.[16, 20-22] As the current biodegradable MNs have mainly been composed of water-soluble polymers, cellulose and polysaccharide materials,[23-26] self-setting ceramics could offer a promising new alternative.

This study aimed to develop and evaluate CaS-based and CaP-based self-setting ceramic microneedle (SCMN) arrays with the ability to hold a wide range of drug amounts, using micromolding under mild conditions. The goal was to control the release rate of the drug from the SCMNs by changing easily adjusted aspects of the design, such as the needle dimensions, the porosity and degradation of the ceramic material, and the interaction between the material and the drug molecules. In this study, the focus was to study the release of small molecule drugs by SCMNs.

Material and Methods

Materials

β-Tricalcium phosphate $(Ca_3(PO_4)_2)$, monocalcium phosphate monohydrate $(Ca(H_2PO_4)_2 \cdot H_2O)$, calcium sulfate alpha hemihydrates $(CaSO_4 \cdot 0.5H_2O)$ and citric acid was used to form the self-setting ceramics Zolpidem tartrate (Cambrex, USA) was used as model drug.

Characterization of self-setting ceramics

The material properties of the self-setting ceramics calcium sulfate dihydrate (CaS) and brushite (CaP) were examined. Information on their crystal structure was obtained using D8 ADVANCE (Brucker AXS GmbH, Germany).). The surface area of the materials were estimated from the N_2 sorption isotherm by

Brunauer–Emmett–Teller (BET) theory, which was performed by
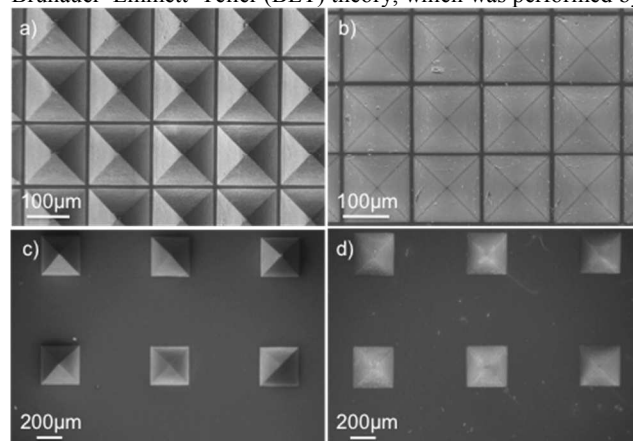

Figure 2 master mold (a and c) and positive replicate (b and d)

Micromeritics ASAP 2020 (Norcross, USA). The compressive strength was tested using an Autograph AGS-H universal testing machine (Shimadzu Corp., Japan) on CaS and CaP rods (r=3mm, H=12 mm). A micro-indentation (Micromet®2100 series, Buehler, USA) was used to measure the hardness of the selected bioceramics. Under a load level of 100gf, the hardness was determined by the average of five repeats. The zeta potential of the ceramic powder suspensions was measured in a Zetasizer Nano ZS (Malvern Instruments, USA).

Preparation and characterization of ceramic microneedles

The pyramid-shaped master mold was developed on a silicon wafer by microfabrication and embossed into a positive replicate using silicone rubber, see **Figure 2**. The mold was then filled with ceramic pastes and processed under vacuum (100 μMPa) to ensure complete filling. The micro-molding process for fabricating the SCMNs is illustrated in **Figure 1**b. The final product was a plate with protruding microneedles. CaP samples were prepared by mixing β-tricalcium phosphate (45 wt%), monocalcium phosphate monohydrate (55 wt%) and 0.5 M citric acid aqueous solution in a liquid/powder ratio of 0.4 and curing the mixture in humid conditions at 37°C for 48 hours. CaS samples were prepared by mixing calcium sulfate hemihydrate with water in a liquid/powder ratio of 0.4 and curing the paste under ambient humidity and temperature. All samples were stored in ambient condition for 24 hours before testing. Scanning electron microscopic (SEM) images of the needles were obtained using a Leo 1550 FEG microscope (Zeiss, UK). The 3D image of the needle array was obtained from the reconstruction of the projections acquired by micro-computed tomography (microCT; Brucker AXS GmbH, Germany).

Verification of the drug release from SCMN

Zolpidem tartrate, an insomnia medication, was used in the study as a model drug for the safety reasons during handling. Zolpidem tartrate is a weak base, which was chosen since 75% of all drugs are weak bases.[27] The drug, zolpidem tartrate, was loaded by two methods. In the first method, the drug was mixed with the raw materials (drug concentration: 1.14 wt% or 2.25 wt%) and the mixture was then cured as above. By this type of drug loading methods, drug molecules were encapsulated in both needles and

the backing layer. In the second method, a 200 µl ethanol solution of zolpidem (5 mg ml^{-1}) was applied to the cured MN plate, which was then dried for 24 hours. The extent of drug release was tested using a bench-top method that provided the in vitro release

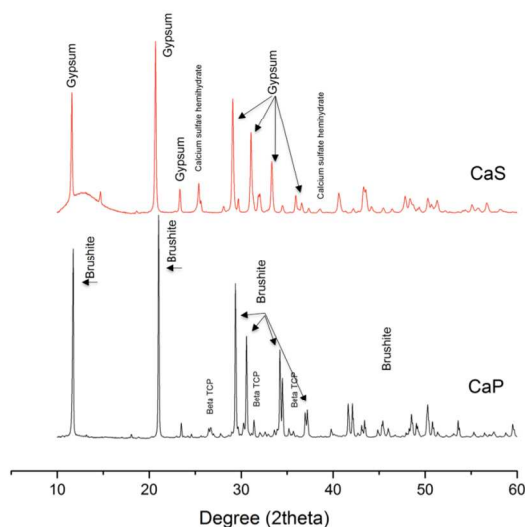5 profile under similar limited humidity to that of commonly used
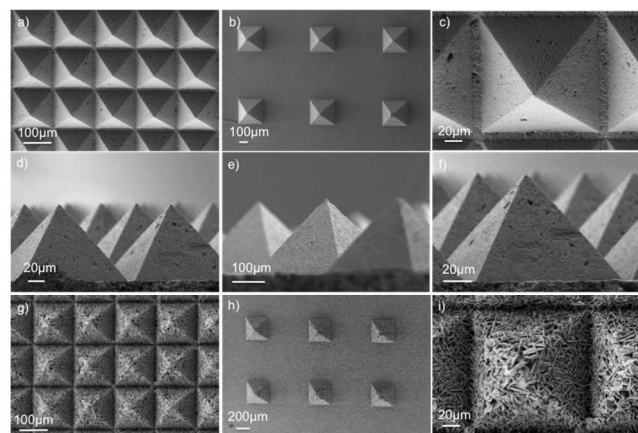Figure 3 X-ray diffraction patterns for CaS and CaP.

Figure 4 SEM images: top view of intact calcium sulfate (CaS) microneedles (MNs): densely arranged (a), sparsely arranged (b), and highly magnified densely arranged needles (c); cross-section view of CaS
10 MNs: densely arranged (d); sparsely arranged (e) and and magnified densely arranged needles (f); intact calcium phosphate (CaP) MNs: densely arranged (g), sparsely arranged (h) and highly magnified (i).

transdermal applications.[28] An MN plate was placed on a piece of moisturized cellulose material. The released drug was collected
15 on the material, which was replaced after 2, 4, 6, 24 and 48 hours. The drug-containing cellulose material was then soaked in HCl solution at pH 1 to release all the collected drug. The drug concentration was measured by a UV/VIS spectrophotometer (Shimadzu 1800, Japan). All tests were performed in triplicate;
20 the error bar denotes the standard deviation of three repeats.

In vitro insertion test

An in vitro insertion test was performed by manually inserting CaP SCMNs into porcine skin samples. The SCMNs was coated with a red hydrophobic dye on the needle tips and inserted

25 manually into porcine skin. The needles were fixed in the skin after insertion and subsequently examined by microCT (Brucker AXS GmbH, Germany).

Results and discussion

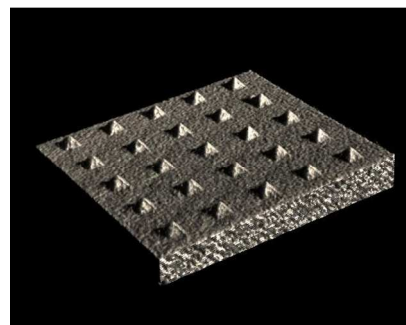### Characterization of self-setting ceramics

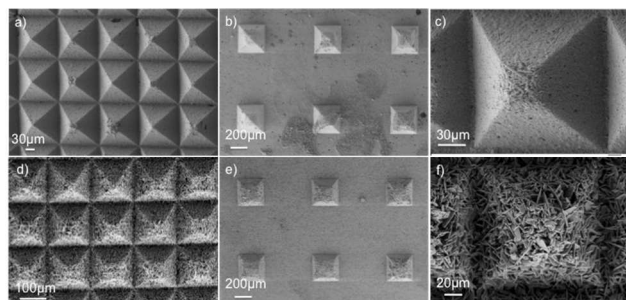30 Figure 5 3-D reconstruction of microtomography images.

Figure 6 SEM images: top view of calcium sulfate (CaS) microneedles (MNs) after release tests: densely arranged (a), sparsely arranged (b), and highly magnified densely arranged needles (c); top view of calcium phosphate (CaP) microneedles (MNs) after release tests: densely arranged
35 (d), sparsely arranged (e), and highly magnified densely arranged needles (f).

The x-ray diffraction pattern showed that the cured CaS and CaP formed crystal structures with little residue of raw materials (**Figure 3**). The surface area of CaS, calculated from the N$_2$
40 soprtion isotherm, was 27.1 m^2 g^{-1}, while that of CaP was 6.0 m^2 g^{-1}. The average compressive strength (six repeats) was 25.7 MPa (SD= 3.8) for CaS and 24.8 MPa (SD= 2.2) for CaP. The hardness of CaP and CaS was 951.3 and 872.8 MPa respectively. The average zeta potentials of CaS and CaP suspensions in 0.05
45 M NaCl solution at pH 6.8 were -15.74 mV (SD=1.79, n=25) and -16.184 mV (SD=2.2, n=25), respectively. The standard specification of acrylic bone cement, including CaS and CaP, suggests that the mechanical strength should be evaluated after 24 hours following the initial mixing.[29, 30] Moreover, the change in
50 porosity would cause obvious effects on mechanical strength.[29] Therefore, we think the storage time of 24 hours, in this study would have insignificant effect on the mechanical strength and the porosity of the self-setting ceramics.

Preparation and characterization of SCMN

55 An outline of the production process for the SCMNs is illustrated in **Figure 1**b. Two types of needles, each with different dimensions, were designed: densely arranged pyramids 100µm in height, 150µm in base width and 160µm between tips (**Figure 4**a

and g); and sparsely arranged pyramids 200μm in height, 285μm in base width and 820μm between tips (**Figure 4**b and h). As observed under SEM, the needle shape was successfully developed and retained when either CaS or CaP was used (**Figure 4**a-b and g-h). More topologic features of the needles were revealed under magnification and cross-section view by SEM (**Figure 4**c, d-f and i) and by the 3-D image reconstructured from the projections obtained by microCT (**Figure 5**). Apart from some small voids on the surface, CaS was densely packed into pyramids with distinct edges and tips. In contrast, CaP crystal plates were loosely stacked, with resultant abundant micrometer-sized pores and channels, to form coarse pyramids. These differences in microstructure characteristics between CaS and CaP SCMNs offer potential for different drug-release profiles.
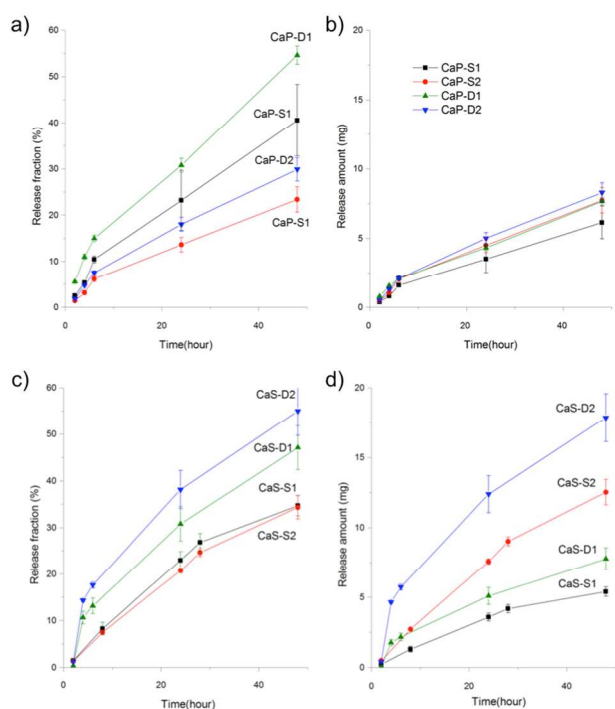
Figure 7 (a) Fraction of drug released versus time and (b) amount of drug released versus time from CaP SCMNs with zolpidem tartrate integrated in the matrix. (c) Fraction of drug released versus time and (d) amount of drug released versus time for CaS SCMNs with zolpidem tartrate integrated in the matrix. CaP = calcium phosphate; CaS = calcium sulphate; D = densely arranged needles; S = sparsely arranged needles; D1 or S1 = needles containing 1.14 wt% zolpidem; D2 or S2 = needles containing 2.25 wt% zolpidem; SCMN = self-setting ceramic microneedle.

Verification of the drug release from SCMN

After 48 hours under drug-release conditions, though two-thirds of the needles were still intact (**Figure 6**a-b and d-e), some needle tips were lost from both CaS and CaP SCMNs (**Figure 6**c and f). Some re-crystallization was observed on the tip and base surfaces of the CaS MNs (**Figure 6**b and e). Many published studies have indicated that ceramic materials can be resorbed,[16, 20, 21] and resorption was thus assumed to be a possible reason for the loss of the bioceramic needle tips, along with abrasion. However, no resorption of alumina MNs has been observed after drug release in previous studies.[13] Needles that are made of biodegradable material could have the potential to reduce the risk of skin irritation and other side effects if the needle is accidentally broken and left in the skin.

In the first study, the drug was added to the bioceramic paste and placed into the SCMN mold before hardening. The release rates were measured from the eight SCMNs investigated: CaS or CaP, using two needle dimensions (sparsely arranged, denoted as -S, or densely arranged, denoted as -D) and two drug concentrations: 1.14 wt% and 2.25 wt% (denoted as 1 and 2, respectively). The rate of release was not affected by the sampling rate during the tests (**Figure 7**b and d), indicating that the decreasing concentration gradient in the drug reservoir of the used testing method did not affect the drug release rate for the SCMNs. As both needles and the backing layer contained drug molecules, the SCMNs with higher drug content could have larger amount of drug left in the backings. Therefore, the SCMNs with lower drug content showed higher release fraction than the ones with higher drug content.

Overall, the results showed that drug release from CaP MNs was slower than that from CaS MNs (**Figure 7**b and d). Because CaS and CaP have similar zeta potentials, it was assumed that the faster release from CaS SCMNs was not associated with a drug-matrix electrostatic interaction. It is suggested that the difference in release rates was the result of differences in the degradation of the ceramic material and the difference in porosity and pore size distribution. CaS has a higher solubility in water compared to CaP (0.24 and 0.088 mg/L, respectively) and has, in a previous study, shown to degrade faster than CaP in vivo,[31] it is to be expected that the CaS MNs would erode more during the drug release test. The SEM pictures taken before and after the drug release test corroborated this theory (**Figure 4**a-i and **Figure 6**a-f). The surfaces on the CaS needles were rougher after the release test, while those on the CaP needles did not show any obvious change. Moreover, the faster degradation rate of CaS resulted in a more obvious variance in the drug release rate from different CaS MNs: from 5.39mg to 17.85mg was released after 48 hours (**Figure 7**d). In contrast, there were no significant differences in the rate of release from the CaP MNs: from 6.13mg to 8.28 mg of zolpidem was released after 48 hours (**Figure 7**b).

The SCMNs with densely arranged needles generally released a higher fraction of the drug content than the sparsely arranged needles (**Figure 7**a and c). This was partly the result of the greater contact area in the densely arranged needles, since the ratio of the bulk surface area of densely and sparsely arranged microneedles was 1.52:1. Additionally, because the erosion occurred mainly on the needle tips (**Figure 6**a-b and d-e), the denser MN array with more needles was subject to more erosion, increasing the bulk surface area and thus promoting drug release.

In most cases, the fraction released from the SCMNs decreased with an increase in original drug content (**Figure 7**a and c). The inverse relationship between release rate and drug content indicates that the release was not exclusively dependent on the dissolution rate of the drug. An increase in bulk surface area will limit the diffusion rate and this could have slowed the release of drug from the matrix. The porosity of the ceramics could also have influenced the release rate. Previous studies have found that the release kinetics of CaP and CaS can be controlled by altering the interconnecting pores and channels.[15, 19] Erosion of the needle tips would probably also have contributed to the drug release. The high release rate from CaS-D2 might have been the result of

the observed extensive erosion. Since drug release from the SCMNs was affected by 1) the total bulk surface area, 2) porosity, and 3) degradation rate of the matrix, these parameters offer potential for controlling the release rate of future SCMNs.

5 Despite the differences in materials and the dimensions of the needles, all the SCMN samples released <6% of the drug content during the first two hours. This may have resulted from the ability of the dry ceramic material to absorb water. The solution would have penetrated into the matrix and then been retained in the 10 pores and channels. The drug molecules dissolved in the trapped aqueous solution would subsequently not have been able to diffuse from the ceramic matrix until excess water was present. The adsorption of water, therefore, could have resulted in to the slow release of drug from the MNs in the first two hours. In 15 addition, subsequent fast diffusion of drug through the trapped solution could have resulted in small bursts of drug release, as seen with the densely arranged CaS MNs between 2 and 4 hours (**Figure 7**c).

The SCMNs that had 1mg of zolpidem tartrate added to the 20 array surface after curing were also evaluated by the *in vitro*
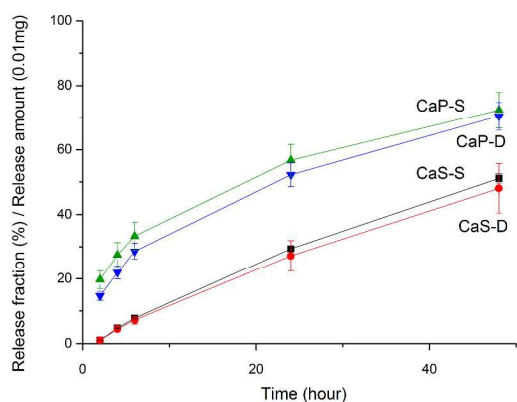

Figure 8 Fraction and amount of drug released versus time for CaP and CaS SCMNs that had been coated with 1mg zolpidem tartrate. CaP = calcium phosphate; CaS = calcium sulphate; D = densely arranged needles; S = sparsely arranged needles.

25 release method. In this case, the drug was released from the CaP MNs faster than from the CaS MNs, which was the opposite result to that seen when the drug was mixed into the ceramic (**Figure 8**). Interestingly, the release rate was not significantly influenced by the density of the needles when the drug was added 30 post hoc. It is possible that the drug solution penetrated into the pores and channels of the ceramic surface to be adsorbed onto the surfaces of the deep microstructures. The more densely packed, compact CaS microstructure might thus have hindered the release of drug from the nanometer pores. In contrast, the spaces between 35 the loosely packed crystal plates in the CaP MNs (**Figure 4**i) would allow moisture to diffuse rapidly into the ceramic structure, thus releasing the drug molecules from the pore surface more easily.

Since the drug is more accessible on the surface of the needles, 40 coated MNs commonly release most of the drug content immediately they come into contact with the medium. However, in this case, it was interesting that there was no dose-dumping effect for any of the SCMNs. It is possible that penetration of the

drug solution into the deep structure resulted in the extended-45 release behavior; i.e. the drug molecules that penetrated deeper inside the matrix were released subsequently. The extended-release behavior could also have resulted from an electrostatic interaction between the negative-charged ceramic surface and the partially positive-charged zolpidem molecules at neutral pH. This 50 electrostatic force only occurs between these ceramics and the molecules that are positively charged at neutral pH.

In vitro **insertion test**

The porcine skin after insertion is shown in **Figure 9**a. The CaP SCMN array remained tightly inserted into the skin, despite some 55 air bubbles (**Figure 9**d). Due to the amount of air bubble existed in between skin and microneedles, (indicated by the arrow in **Figure 9**d) the contrast between air, microneedles and skin is not obvious. The pyramid shape was mostly retained (**Figure 9**b and c) and no breakages were seen. The reconstruction of the 60 microCT images showed that the skin tissue was not compressed under the needles, indicating that the needles had pierced the skin (**Figure 9**d). The results suggested that the CaP SCMNs had
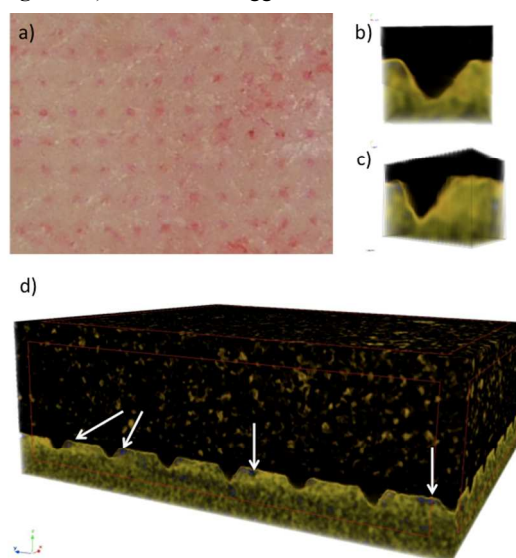

Figure 9 a) Image of the porcine skin after insertion of CaP SCMN. b), c) and d) Three-dimensional reconstruction of a microtomography image of 65 insertion of self-setting ceramic microneedles (SCMNs) into porcine skin samples. b) Front-on view of a single needle penetrating into the skin with no sign of breakage or erosion. The needle tip remained intact after insertion. c) Side-on view of a single needle inserted into the skin. d) The interface between the SCMNs and the skin. The SCMN plate is colored 70 dark brown, the porcine skin is colored yellow, and air is colored blue and indicated by arrows.

adequate mechanical strength to allow manual insertion. This type of mechanically strong MNs, which have the ability to be resorbed by the interstitial fluid, could provide successful drug 75 delivery through the skin and reduce the risk of skin irritation caused by residual needle material.

Biodegradable MNs have recently received considerable attention because of their good biocompatibility, drug loading capacity, controlled-release behaviour, and potential for safe 80 disposal, comparing to solid MNs.[10] Resorbable bioceramics, made using a micromolding procedure from self-setting CaS (gypsum) or CaP (brushite) as outlined here, appear to be good

candidate materials for MNs. The manufacturing procedure, performed under mild conditions, has the potential to avoid damage to the loaded drug molecules from extreme temperatures or pH levels. The self-setting ceramics also had adequate mechanical strength to ensure the successful insertion of the MNs into skin. The results show that the contact area between the MNs and the skin was the influential factor for the rate of drug release. The porosity and resorbability of the self-setting ceramics can be used to regulate the release behavior. Moreover, the method of drug loading can also influence the rate of drug release.

In future studies, the shape of the needles should be optimized to allow easier and more effective insertion and sustained drug release. The optimum length and shape of MNs to allow easier insertion and constant drug release has been studied in detail previously.[32-34] Because the nature of our study was proof-of-concept, only two needle dimensions were investigated. It is suggested that optimization of the needle shape and increasing the sharpness of the needles could improve the performance of the SCMNs.

Conclusion

In conclusion, two SCMNs containing easily adjustable drug doses were manufactured using a simple micromolding process under mild conditions, and evaluated. The two drug loading processes did not affect the drug's properties. The release rates of the drug from the MNs were able to be altered by changing the bulk surface area, porosity and resorbability of the ceramics. Self-setting bioceramics appear to be a promising material for MN applications.

Acknowledgements

Notes and references

a Division for Applied Materials Science, Department of Engineering Sciences, The Ångström Laboratory, Uppsala University, Box 534, SE-751 21 Uppsala, Sweden; Fax: +46-18-471 35 72 Tele: +46-18-471 30 65 E-mail: wei.xia@angstrom.uu.se

1. M. R. Prausnitz, *Advanced Drug Delivery Reviews*, 2004, **56**, 581-587.
2. K. van der Maaden, W. Jiskoot and J. Bouwstra, *Journal of Controlled Release*, 2012, **161**, 645-655.
3. Y.-C. Kim, J.-H. Park and M. R. Prausnitz, *Advanced Drug Delivery Reviews*, 2012, **64**, 1547-1568.
4. S. M. Bal, J. Caussin, S. Pavel and J. A. Bouwstra, *European Journal of Pharmaceutical Sciences*, 2008, **35**, 193-202.
5. H. S. Gill, D. D. Denson, B. A. Burris and M. R. Prausnitz, *The Clinical journal of pain*, 2008, **24**, 585-594.
6. Y. A. Gomaa, L. K. El-Khordagui, M. J. Garland, R. F. Donnelly, F. McInnes and V. M. Meidan, *Journal of Pharmacy and Pharmacology*, 2012, **64**, 1592-1602.
7. E. V. Mukerjee, S. D. Collins, R. R. Isseroff and R. L. Smith, *Sensors and Actuators A: Physical*, 2004, **114**, 267-275.
8. S. Liu, M. N. Jin, Y. S. Quan, F. Kamiyama, H. Katsumi, T. Sakane and A. Yamamoto, *Journal of controlled release : official journal of the Controlled Release Society*, 2012, **161**, 933-941.
9. M. C. Chen, S. F. Huang, K. Y. Lai and M. H. Ling, *Biomaterials*, 2013, **34**, 3077-3086.
10. T.-M. Tuan-Mahmood, M. T. C. McCrudden, B. M. Torrisi, E. McAlister, M. J. Garland, T. R. R. Singh and R. F. Donnelly, *European Journal of Pharmaceutical Sciences*, 2013, **50**, 623-637.
11. R. S. Byrne and P. B. Deasy, *International Journal of Pharmaceutics*, 2002, **246**, 61-73.
12. S. Bystrova and R. Luttge, *Microelectronic Engineering*, 2011, **88**, 1681-1684.
13. M. Verhoeven, S. Bystrova, L. Winnubst, H. Qureshi, T. D. de Gruijl, R. J. Scheper and R. Luttge, *Microelectronic Engineering*, 2012, **98**, 659-662.
14. M. Shirkhanzadeh, *J Mater Sci: Mater Med*, 2005, **16**, 37-45.
15. M. P. Ginebra, T. Traykova and J. A. Planell, *Journal of Controlled Release*, 2006, **113**, 102-110.
16. F. Theiss, D. Apelt, B. Brand, A. Kutter, K. Zlinszky, M. Bohner, S. Matter, C. Frei, J. A. Auer and B. von Rechenberg, *Biomaterials*, 2005, **26**, 4383-4394.
17. M. P. Hofmann, A. R. Mohammed, Y. Perrie, U. Gbureck and J. E. Barralet, *Acta Biomaterialia*, 2009, **5**, 43-49.
18. M. A. Rauschmann, T. A. Wichelhaus, V. Stirnal, E. Dingeldein, L. Zichner, R. Schnettler and V. Alt, *Biomaterials*, 2005, **26**, 2677-2684.
19. S. Hesaraki, F. Moztarzadeh, R. Nemati and N. Nezafati, *Journal of Biomedical Materials Research Part B: Applied Biomaterials*, 2009, **91B**, 651-661.
20. A. Oberle, F. Theiss, M. Bohner, J. Muller, S. B. Kastner, C. Frei, I. Boecken, K. Zlinszky, S. Wunderlin, J. A. Auer and B. von Rechenberg, *Schweizer Archiv fur Tierheilkunde*, 2005, **147**, 482-490.
21. M. Bohner, *Materials Today*, 2010, **13**, 24-30.
22. D. Stubbs, M. Deakin, P. Chapman-Sheath, W. Bruce, J. Debes, R. M. Gillies and W. R. Walsh, *Biomaterials*, 2004, **25**, 5037-5044.
23. P. S. Sean, G. K. Dimitrios, M. Maria del Pilar, L. Jeong Woo, Z. Vladimir, O. C. Seong, M. Niren, W. C. Richard, S. Ioanna and R. P. Mark, *Nature medicine*, 2010, **16**, 915-920.
24. L. Y. Chu and M. R. Prausnitz, *Journal of Controlled Release*, 2011, **149**, 242-249.
25. K. Lee, C. Y. Lee and H. Jung, *Biomaterials*, 2011, **32**, 3134-3140.
26. M. G. McGrath, S. Vucen, A. Vrdoljak, A. Kelly, C. O'Mahony, A. M. Crean and A. C. Moore, *European Journal of Pharmaceutics and Biopharmaceutics*.

27. M. E. Aulton, *Aulton's pharmaceutics : the design and manufacture of medicines*, 3rd edn., Churchill Livingstone, Edinburgh ; New York, 2007.

28. B. Cai, #xf6, K. derkvist, H. Engqvist, #xe5, kan and S. Bredenberg, *Pain Research and Treatment*, 2012, **2012**, 6.

29. F. Tamimi, Z. Sheikh and J. Barralet, *Acta Biomater*, 2012, **8**, 474-487.

30. A. International, www.astm.org, West Conshohocken, PA, Editon edn., 2008.

31. N. Eliaz, *Degradation of implant materials*, Springer, 2011.

32. O. Olatunji, D. B. Das, M. J. Garland, L. Belaid and R. F. Donnelly, *Journal of pharmaceutical sciences*, 2013, **102**, 1209-1221.

33. B. Al-Qallaf, D. B. Das and A. Davidson, *Asia-Pacific Journal of Chemical Engineering*, 2009, **4**, 845-857.

34. S. D. Gittard, B. Chen, H. Xu, A. Ovsianikov, B. N. Chichkov, N. A. Monteiro-Riviere and R. J. Narayan, *Journal of Adhesion Science and Technology*, 2012, **27**, 227-243.